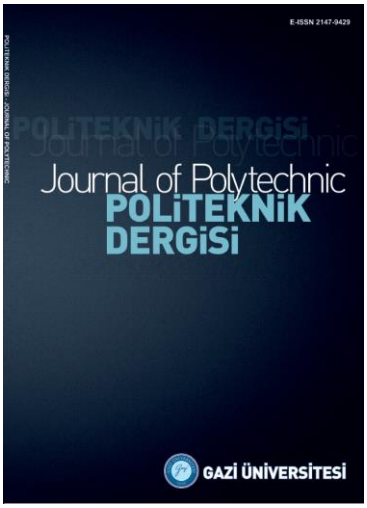

POLİTEKNİK DERGİSİ

JOURNAL of POLYTECHNIC

ISSN: 1302-0900 (PRINT), ISSN: 2147-9429 (ONLINE)
URL: http://dergipark.org.tr/politeknik

Mosaic defects of AlN buffer layers in GaN/AlN/4H-SiC epitaxial structure

GaN/AlN/4H-SiC epitaksiyel yapının AlN tampon tabakasının mozaik kusurları

***Yazar(lar) (Author(s))**: Tuğçe ATAŞER[1], Durmuş DEMİR[2], A. Kürşat BİLGİLİ[3], M. Kemal ÖZTÜRK[4], Süleyman ÖZÇELİK[5]*

ORCID[1]: 0000-0002-8146-7707

ORCID[2]: 0000-0003-2446-9279

ORCID[3]: 0000-0003-3420-4936

ORCID[4]: 0000-0002-8508-5714

ORCID[5]: 0000-0002-3761-3711

Bu makaleye şu şekilde atıfta bulunabilirsiniz(To cite to this article): Ataşer T., Demir D., Bilgili A. K., Öztürk M. K., Özçelik S., "Mosaic defects of AlN buffer layers in GaN/AlN/4H-SiC epitaxial structure", ***Politeknik Dergisi***, 24(2): 511-516, (2021).

Erişim linki (To link to this article): http://dergipark.org.tr/politeknik/archive

DOI: **10.2339/politeknik.682649**

Mosaic Defects of AlN Buffer Layers in GaN/AlN/4H-SiC Epitaxial Structure

Highlights

- *Structural properties of AlN buffer layers are investigated by (HR-XRD) technique.*
- *Interfacial roughness of AlN buffer layer was determined by XRR technique.*

Graphical Abstract

Structural properties of AlN buffer layers, grown by Metal Organic Chemical Vapor Deposition (MOCVD) on 4H-SiC substrate with thicknesses of 61.34, 116.88, 129.46 and 131.50 nm, are investigated by High Resolution X-Ray Diffraction (HR-XRD) technique. Interfacial roughness of AlN buffer layer was determined by XRR technique.

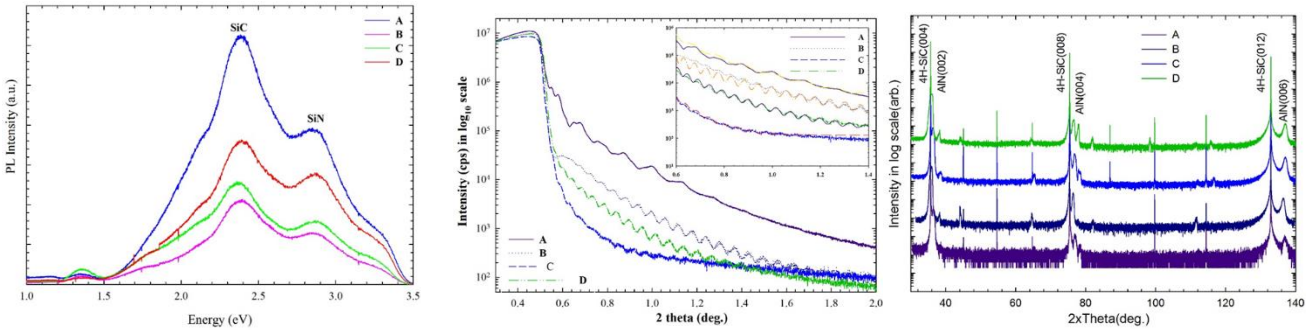

Figures Photoluminescene (PL) as a function of emission energy for all the investigated AlN buffer samples/ Specular x-ray reflectivity of AlN buffer layers/ High resolution Bragg reflections curves of (002), (004) and (006) planes of samples A, B, C and D.

Aim

The aim of this study is to investigate Mosaic Defects of AlN Buffer Layers in GaN/AlN/4H-SiC Epitaxial Structure

Design & Methodology

Structural properties of AlN buffer layers, grown by Metal Organic Chemical Vapor Deposition (MOCVD) on 4H-SiC substrate with thicknesses of 61.34, 116.88, 129.46 and 131.50 nm, are investigated by High Resolution X-Ray Diffraction (HR-XRD) technique. Interfacial roughness of AlN buffer layer was determined by XRR technique.

Originality

This study is original because AlN buffer layer is rarely used with GaN.

Findings

The interface roughness value of 131.50 nm thick sample is determined as 0.50 nm. Mosaic defects, tilt angle, vertical and lateral coherence lengths are characterized by HR-XRD technique. The edge and screw dislocations of the 131.50 nm thick sample are found as 2.98x1010 and 8.86x108 cm^{-2} respectively.

Conclusion

HR-XRD and XRR results showed that the thickest sample (131.50 nm) is more capable of preventing diffusion of dislocations to GaN layer.

Declaration of Ethical Standards

The author(s) of this article declare that the materials and methods used in this study do not require ethical committee permission and/or legal-special permission.

Mosaic Defects of AlN Buffer Layers in GaN/AlN/4H-SiC Epitaxial Structure

Araştırma Makalesi / Research Article

Tuğçe ATAŞER[1*], Durmuş DEMİR[2], A. Kürşat BİLGİLİ[2*], M. Kemal ÖZTÜRK[1,2], Süleyman ÖZÇELİK[1,2]

[1]Photonics Application and Research Center, Gazi University, 06500, Ankara, Turkey

[2]Department of Physics, Faculty of Science, Gazi University, 06500, Ankara, Turkey

(Geliş/Received : 31.01.2020 ; Kabul/Accepted : 22.04.2020)

ABSTRACT

Structural properties of AlN buffer layers, grown by Metal Organic Chemical Vapor Deposition (MOCVD) on 4H-SiC substrate with thicknesses of 61.34, 116.88, 129.46 and 131.50 nm, are investigated by High Resolution X-Ray Diffraction (HR-XRD) technique. Interfacial roughness of AlN buffer layer was determined by XRR technique. The interface roughness value of 131.50 nm thick sample is determined as 0.50 nm. Mosaic defects, tilt angle, vertical and lateral coherence lengths are characterized by HR-XRD technique. The edge and screw dislocations of the 131.50 nm thick sample are found as $2.98x10^{10}$ and $8.86x10^{8}$ cm^{-2} respectively. The results indicate that 131.50 nm thick AlN buffer layer should be used in order to gain high performance in optoelectronic terms in this study. Thus, optimization of AlN buffer layer thickness is extremely important in device performance.

Keywords: MOCVD, AlN, HR-XRD, XRR, mosaic defect.

GaN/AlN/4H-SiC Epitaksiyel Yapının AlN Tampon Tabakasının Mozaik Kusurları

ÖZ

Metal Organik Kimyasal Buhar Biriktirme (MOCVD) yöntemiyle 4H-SiC alttaşın üzerine 61.34, 116.88, 129.46 ve 131.50 nm kalınlıklarında büyütülen AlN tampon tabakaların yapısal özellikleri yüksek çözünürlüklü X-ışını kırınımı (HR-XRD) tekniği ile incelendi. AlN tampon tabakanın arayüz pürüzlülüğü XRR tekniği ile belirlendi. 131.50 nm kalınlığındaki numunenin arayüz pürüzlülüğü 0.50 nm olarak bulundu. Mozaik kusurlar, eğim açısı, düşey ve yatay koherens uzunlukları HR-XRD tekniği ile karakterize edildi. 131.50 nm kalınlığındaki numunenin kenar ve vida tipi dislokasyonları sırasıyla $2.98x10^{10}$ ve $8.86x10^{8}$ cm^{-2} olarak hesaplandı. Bu sonuçlar gösterdi ki bu çalışmada optoelektronik olarak yüksek performans elde edebilmek için 131.50 nm kalınlığında AlN tampon tabaka tercih edilmelidir. AlN tampon tabakanın kalınlığının iyi seçilmesi cihazın performansı açısından son derece önemlidir.

Anahtar Kelimeler: MOCVD, AlN, HR-XRD, XRR, mozaik kusur.

1.INTRODUCTION

Use of materials such as diamond, SiC, III-Nitrides and II-IV group elements which have wide energy band gap in electronic devices, decrease the negative application effects. Among these materials, III-Nitride semiconductors, because of their direct band gaps, they have high absorption coefficients and sharp peaks in PL spectra. Today, III-Nitrides are widely preferred for production of nano-electronic and nano-optoelectronic devices operating under high power, temperature and radiation conditions, because of the properties above [1]. Among compounds formed by III-V group elements such as nitride based GaN and AlN are promising structures for designing optoelectronic devices operating in blue-ultraviolet (UV) spectral range.

Different buffer layers are preferred in Light Emitting Diodes (LEDs), High Electron Mobility Transistors (HEMTs), Solar Cells (SCs) and many other optoelectronic devices because they optimize the properties of active layers [2]. In order to increase device performance, lattice mismatch, dislocation density and difference in thermal expansion coefficients should be minimized. For gaining high crystal quality, buffer layers should be grown on GaN epitaxial layer grown on the substrate. Buffer layer prevents forming of dislocations between the substrate and layers grown on it. Also, buffer layer minimizes lattice mismatch between layers, this situation decreases stress and lattice relaxation. Because of its perfect chemical stability and high thermal conductivity AlN is a preferred buffer layer for growing high quality GaN films on substrates such as sapphire, SiC and Si [3, 4]. AlN and SiC have hexagonal crystal structure and they have similar crystallographic properties such as lattice parameters and thermal expansion coefficients [5]. Because of these common properties, during growth of GaN based thin films on SiC substrate AlN is a convenient buffer layer [6]. In Table 1 crystallographic properties of AlN and SiC can be seen. These universal lattice parameters are taken from pdf

* Sorumlu yazar (Corresponding Author)
e-mail: sunkurt4@gmail.com

251133 and 221317 database. Also in terms of validity of GaN devices high thermal conductivity of SiC is important [7]. In recent studies, it is seen that growing AlN buffer layer between substrate and GaN supports modification of surface morphology of GaN [8].

Table 1. Crystallographic properties of AlN and SiC

Crystalline properties	Index	AlN [9]	4H-SiC [10]
Crystal structure		Wurtsize (hexagonal)	Wurtsize (hexagonal)
Lattice parameter (Å)	a	3.111	3.073
	c	4.9792	10.081

There are many similar studies in literature. For example Deok K. K.[11] investigated effect of AlN buffer layer thickness on structural properties in his work. He also found out that suitable thickness of AlN buffer layer optimize structural properties. H. Marchand and co-workers made another study in (2014) and concluded that use of AlN buffer layer with a suitable thickness prevents dislocations to diffuse[12].

In this study, AlN buffer layers with thicknesses of 61.34, 116.88, 129.46 and 131.50 nm are grown on 4H-SiC substrate by using MOCVD technique. These structures are called as sample A, B, C and D respectively. Structural properties of AlN buffer layers with different thicknesses are investigated. The crystal quality of the buffer layers was investigated by XRR technique. Because nitride based materials crystallize during growth they have mosaic structure defects in general. Defected AlN buffer layers are characterized with tilt angle, lateral and vertical coherence lengths by HR-XRD technique. In order to determine tilt angle of structures.

2.MATERIAL and METHOD

All samples are grown on 4H-SiC substrate by using low pressure MOCVD. For Al and N, Thrimethylaliminium (TMAl) and NH_3 are used as source respectively. H_2 is used as carrier gas. Before growth of AlN, SiC substrates are annealed at 1080 ^oC for 10 minutes in order to remove surface dirt. First 10 nm thick AlN layer is grown under 50 mbar reactor pressure and at 840^oC temperature. Later reactor temperature is increased to 1100, 1020, 970 and 1050^oC for samples A, B, C and D respectively. Main AlN layer is grown under 30, 50, 50 and 30 mbar reactor pressure at 1100, 1020, 970 and 1050^oC temperature respectively. Samples A, B, C and D are grown with 50, 1000, 1000 and 50 sccm NH_3 flux ratios, respectively.
Samples are characterized by HR-XRD measurement. HR-XRD measurements are made with Bruker D8-Discovery high resolution diffractometer using $CuK_{\alpha 1}$ radiation, mirror with production and a 4 bounce Ge(022) monochromator. By using the results of these measurements crystal quality of the samples are determined.

3. RESULTS & DISCUSSION

X-Ray Reflectivity (XRR), is a useful technique for determining the quality of interfaces in a heterostructure [13]. This technique is used for measuring layer thicknesses between 0.1-1 nm, material density smaller than %1-2 and interface roughness between 3-5 nm. In general, these types of analyses makes measurements at nano-scale for crystal and amorphous materials. Fig. 1 shows XRR spectra of AlN buffer layers grown on SiC substrate. Inserted plot in this figure is used for detailing Kiessig finger peaks and fits. Formation of finger peaks indicates that samples have good interface quality. Frequency and width of fluctuations are effected from thickness of hetero structures, interface roughness and differences in the density of layers [14]. As can be seen, sharp dropping point is at about critical angle point 0.6. This dropping point that is critical angle is used for describing density of AlN buffer layer. For all four of the samples sharp dropping points are approximately the same. Different negative slopes in the plot is related with roughness of AlN buffer layer. Roughness values for samples A, B, C and D are measured as 1.12, 1.36, 2.50 and 0.50 nm respectively. Thickness is calculated with $d=\lambda/2\Delta\theta$ equation [15]. Here λ is the wavelength of x-ray source, $\Delta\theta$ is the difference of angles of two finger peaks in radians. This result shows that sample D which is thicker has better GaN thin film interface quality.

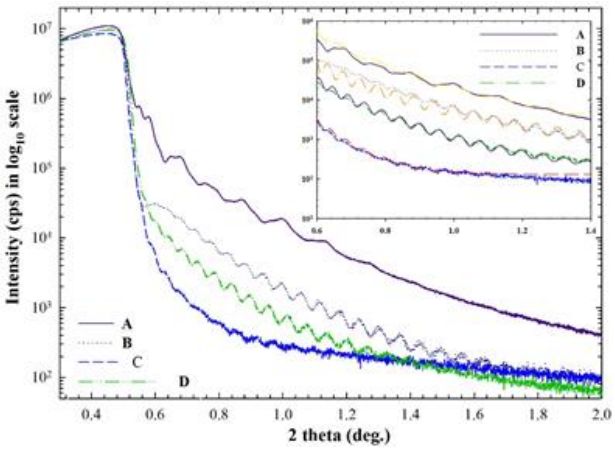

Figure 1. Specular x-ray reflectivity of AlN buffer layers

HR-XRD plot of AlN buffer layers grown on SiC substrate is given in Fig. 2 for four samples. AlN buffer layer peaks can be seen in Fig. 2 for (002), (004) and (006) symmetric planes. These peaks for four samples shows variation in peak widths. This situation is related to mosaic crystal structures. Symmetric plane peaks for AlN buffer layer is given in Table 2. FWHM (Full Width at Half Maximum) values are discussed in Fig. 3. Fig. 3 shows FWHM values of (002), (004) and (006) peaks for AlN buffer layers with different thicknesses. As the thickness of the sample increase FWHM increase and crystal quality decrease. As the thickness increase in samples A and B, FWHM first decreases and after a certain value it increases. An optimum value can be seen

after 40 nm. For B and D samples as the thickness increase, FWHM values increase regularly.

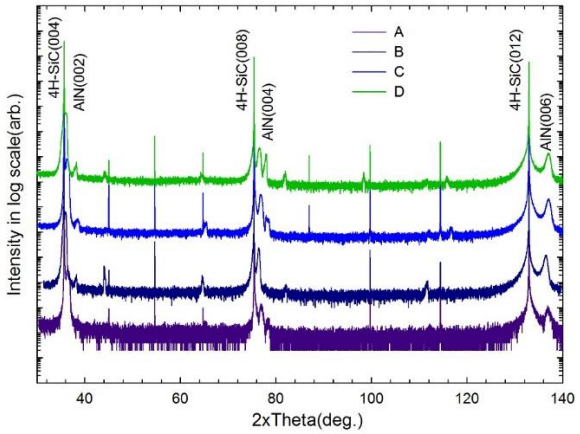

Figure 2. High resolution Bragg reflections curves of (002), (004) and (006) planes of samples A, B, C and D.

Peak positions of AlN buffer layers are gained from rocking curves. In symmetric planes of AlN buffer layers, decreasing lateral coherence lengths and increasing tilt angles results in broadening of vertical rocking curves in pole axis. Broadening of reflection peaks, by the support of tilt angles and coherence lengths, presents a linear dependency for reflection order [15]. In order to calculate tilt angle, lateral coherence length and the edge dislocation and screw dislocation. In symmetric direction, a Williamson Hall (W-H) plot can be used shown in Fig. 4 [16]. W-H plot is gained by drawing FWHMx(sinθ)/λ(x10^{-3}Å^{-1}) versus sinθ/λ(Å^{-1}) linear curve for every reflection. A linear fit is applied to this plot as shown in Fig. 4. Slope of W-H plot gives tilt angle and y-axis intercept of this plot gives lateral coherence

Table 2. AlN symmetrical plane peaks of samples A, B, C and D in degree unit

	A	B	C	D
(002)	36.45	36.06	36.22	36.54
(004)	77.29	77.47	76.83	76.57
(006)	136.82	136.52	137.01	137.11

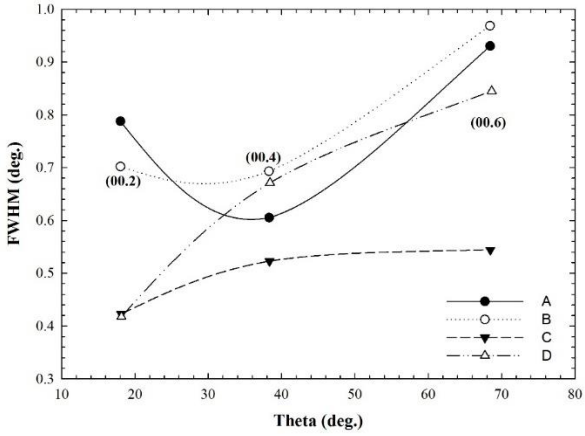

Figure 3. The FWHMs of (00.2) (00.4) (00.6) peaks in AlN buffer layer versus theta

length ($L_{\parallel}$=0.9/(2y_0)). In Fig. 4 W-H plot of samples A, B, C and D for (002), (004) and (006) symmetric planes.

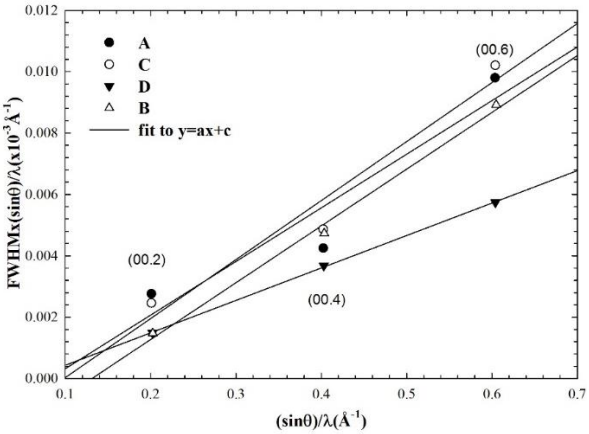

Figure 4. Williamson-Hall plot for AlN layers of different thickness. The ω-2θ scans were measured for (*00.l*)

W-H plot can also be drawn by plotting FWHMx(cosθ)/λ(x10^{-4} Å^{-1}) versus sinθ/λ (Å^{-1}) and a linear fit is applied. In Fig. 5 W-H plot of samples A, B, C and D for (002), (004) and (006) symmetric planes can be seen. Slope of this fit gives mixed strain and y-axis intercept of it gives vertical coherence length. All four samples show negative mixed strain behavior. The heterogeneous strain in 4 samples shows negative parallel behavior. Vertical coherence length is calculated from $L_{\perp}$=(0.9)/(2y_0) equation and mixed strain can be calculated from 4ε [17]. Determined values (the tilt angle, the lateral ($L_{\parallel}$) and vertical coherence ($L_{\perp}$) length, edge dislocation (N_{edge}) and screw dislocation (N_{screw}) and heterogeneous strain ($\varepsilon_{\perp}$)) are presented in Table 3.

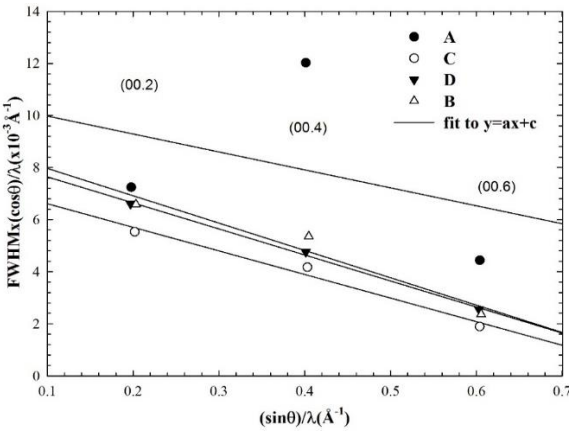

Figure 5. Williamson-Hall plot for AlN layers of different thickness. Here FWHM is the peak broadening of 2θ scans

In Fig. 6 left and right y-axes show lateral and vertical coherence lengths respectively. As can be seen in Figure 6. thickness of samples A, B, C and D are determined as 61.34, 116.88, 129.46 and 131.50 nm respectively. For all four samples, lateral and vertical coherence length values are between 40 and 700 nm. Also, they show

fluctuated behavior dependent on the structure of the samples. As the thickness increase, vertical and coherence length values for samples A, B, C increase but, for sample D they decrease. For sample C in *a*- and *c*-directions crystal size has broadened. However, sample D *a*- direction crystal size has compressed while *c*-direction crystal has broadened. As expected lateral coherence lengths are less than vertical coherence lengths in general. This situation supports *c*-oriented growth in dominant rectangular prism shaped growth.

Table 3. Mosaic structural properties of AlN buffer layer

	A	B	C	D
N_{edge} ($x10^{10} cm^{-2}$)	38.94	8.99	32.78	2.98
N_{screw} ($x10^{8}$ cm^{-2})	7.91	9.57	2.89	8.86
$L_{\perp}$ (nm)	315.62	238.00	721.47	185.54
$L_{\parallel}$ (nm)	42.76	47.64	73.5821	79.46
Tilt(°)	0.017	0.018	0.019	0.010
$\varepsilon_{\perp}$	$-2.86x10^{-3}$	$-2.19x10^{-3}$	$-1.42x10^{-3}$	$-6.29x10^{-4}$

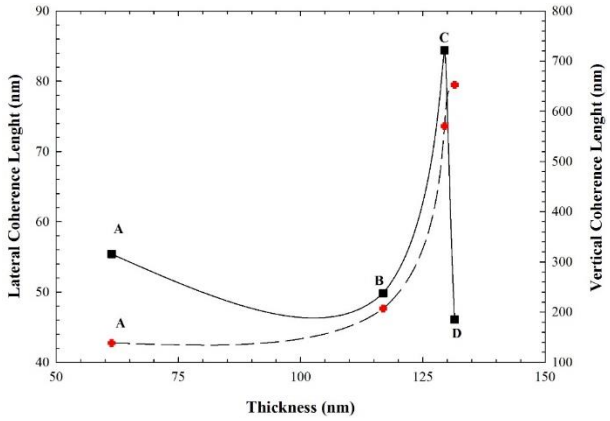

Figure 6. Lateral and vertical coherence lengths of AlN buffer layer versus the thickness

In Fig. 7 thickness versus strain plot can be seen. It is noticed that strain values of the samples are at 10^{-3} level in general. As the thickness of AlN buffer layer increase, strain value decrease. It is seen that as the thickness increase compressed strain increase. Sample D has the least compressed strain value and sample A has the least strain value. This result can be attributed to stoichiometry of AlN buffer layers and density of point defects at layers.

In Fig. 8 left and right y-axes show variation of edge and screw dislocations versus thickness, respectively. Out of plane and in-plane mismatch of crystallites in the layers are related to screw and edge type dislocations respectively [18]. Edge dislocation and screw dislocation can be calculated by using the following equations [19, 20].

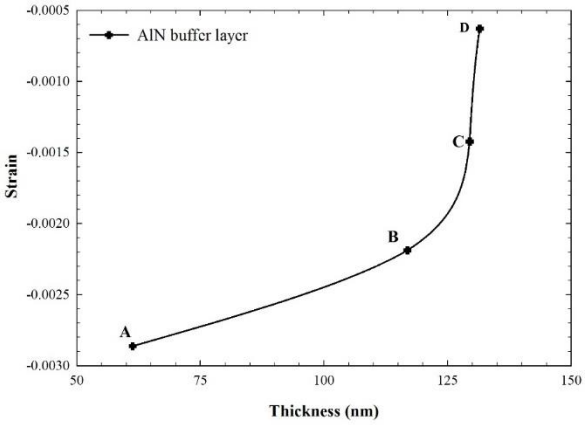

Figure 7. Strain versus the thickness

$$N_{edge} = {FWHM}/{2.1|b_{edge}|L_{\parallel}}$$

$$N_{screw} = {\alpha_{\omega}^{2}}/{4.35|b_{screw}|^{2}}$$

Here α_w is the tilt angle which is a mosaic defect and b_{screw} is the length of Burgers vector. FWHM is the peak broadening of asymmetric planes and b_{edge} is also the length of Burgers vector. $L_{\parallel}$ is the length of lateral coherence length. As expected the value of screw dislocation density for AlN buffer layer is smaller than the value of edge dislocation density [21, 22]. Though there is a decrease in the dislocation densities of the samples by increasing thickness, in sample C there is a radical increase. In screw plot, samples A, B and D are at 10^8 level but in sample C screw dislocation value is smaller. As can be seen in Fig. 8 sample D has the least dislocation density. This result indicates that in order to grow higher quality GaN films, thicker AlN buffer layers should be grown on SiC substrate.

The main reason of variation in defects with thickness of buffer layer is minimization of lattice mismatch. Buffer layers have useful effect on lattice mismatch and the difference in thermal expansion coefficients between the substrate and the material grown on it. If buffer layer is not used or misused with a wrong thickness, there may occur cracks or crack-like defects in the structure. This situation may result with mulfunction of the device produced.

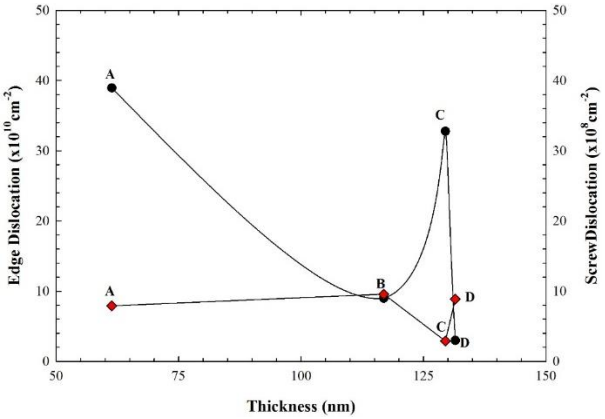

Figure 8. The FWHMs of (00.2) (00.4) (00.6) peaks in AlN buffer layer versus theta

4. CONCLUSION

AlN buffer layers with thicknesses of 61.34, 116.88, 129.46 and 131.50 nm are grown on 4-H SiC substrate by using MOCVD technique. Structural properties of the samples are investigated with HR-XRD technique. According to HR-XRD results, effect of thickness on lateral and vertical coherence lengths, screw and edge type dislocations of AlN buffer layers are investigated. Screw type dislocation density for AlN buffer layer is found between $1.41x10^8$ (S.C) and $19.64x10^8$ cm^{-2} (S.A). Edge type dislocation density is found between $2.98x10^{10}$ (S.D) and $56.19x10^{10}$ cm^{-2} (S.A). Samples with 116.88 and 131.50 nm thickness have the least dislocation density. Interface roughness of AlN buffer layers is determined from XRR technique. It is found that sample with 131.50 nm thickness has the least interface roughness. HR-XRD and XRR results showed that the thickest sample (131.50 nm) is more capable of preventing diffusion of dislocations to GaN layer. This result is valid only for samples used in this study. Because even a small variation in growth procedure may cause large differences in results gained from structural characterization. Growth method can also effect results as mentioned in results and discussion section and in references [11] and [12]. So the good result gained for 131.50 nm thick AlN buffer layer can not be generalized.

As a result of this study, it is seen that 131.50 nm thick AlN buffer layer is more convenient to reduce dislocations among the samples investigated in this study. Because of this, optimization of AlN buffer layer thickness is important in device performance.

Acknowledgement

This work supported by CSBB in Turkey under the project number 2016K121220.

DECLARATION OF ETHICAL STANDARDS

The author(s) of this article declare that the materials and methods used in this study do not require ethical committee permission and/or legal-special permission.

AUTHORS' CONTRIBUTIONS

Tugce ATASER: Perofrmed the experiments and analyse the results.

Durmus. DEMIR: Perofrmed the experiments and analyse the results.

A.Kürşat. BILGILI: Wrote the manuscript.

M Kemal OZTURK: Checked the analyse results

Suleyman OZCELIK: Checked the whole manuscript before submission**.**

CONFLICT OF INTEREST

There is no conflict of interest in this study.

REFERENCES

[1] Morkoç H., Cingolania R., Gil B., "Polarization effects in nitride semiconductor device structures and performance of modulation doped field effect transistors", ***Solid-State Electronics,*** 43: 1753-1771, (1999).

[2] Prazmowska J., Korbutowicz R., Wosko M., Paszkiewicz R., Kovac J., Srnanek R., Tłaczała M., "Influence of AlN Buffer Layer Deposition Temperature on Properties of GaN HVPE Layers", ***Acta Physica Polonica A***, 116: 123-125, (2009).

[3] Lan Y., Chen L., Cao G., Xu L., Xun D., Xu T., Liang J., "Low-temperature synthesis and photoluminescence of AlN", ***Journal of Crystal Growth,*** 207: 247-250, (1999).

[4] Cao G., Chen L., Lan Y., Li J., Xu Y., Xu T., Liu Q., Liang J., "Blue emission and Raman scattering spectrum from AlN nanocrystalline powders", ***Journal of Crystal Growth,*** 213: 198-202, (2000).

[5] Ponce F., Van de Walle C., Northrup J., "Atomic arrangement at the AlN/SiC interface", ***Physical Review B,*** 53: 7473-7478, (1996).

[6] Ponce F., Krusor B., Major S., Plano W., Welch D., "Microstructure of GaN epitaxy on SiC using AlN buffer layers", ***Applied Physics Letters,*** 67: 410-412, (1995).

[7] Huang W., Chu C., Wong Y., Chen W., Lin K., Wu H., Lee W., Chang E., "Investigations of GaN growth on the sapphire substrate by MOCVD method with different AlN buffer deposition temperatures", ***Materials Science in Semiconductor Processing,*** 45: 1-8, (2016).

[8] Brubaker M., Levin I., Davydov V., Rourke D., Sanford N., Bright V., Bertness K., "Effect of AlN buffer layer properties on the morphology and polarity of GaN nanowires grown by molecular beam epitaxy", ***Journal of Applied Physics***, 110: 053506-1-7, (2011).

[9] Singh N., Berghmans A., Zhang H., Wait T., Clarke R., Zingaro J., Golombeck J., "Physical vapor transport growth of large AlN crystals", ***Journal of Crystal Growth,*** 250: 107–112, (2003).

[10] Stockmeier M., Müller R., Sakwe S., Wellmann P., Mager A., "On the lattice parameters of silicon carbide", ***Journal of Applied Physics,*** 105: 033511-4, (2009).

[11] Kiyu D., "Effect of AlN buffer thickness on stress relaxation in GaN layer on Si (1 1 1)", ***Solid State Electronics,*** 51: 7, (2007).

[12] Marchand H., Zhang N., Zhao L., Golan Y., Rosner S., Girolami G., Paul T., Ibbetson J., Keller S., Den Baars S., Speck J., Mishra U., "Structural and optical properties of GaN laterally overgrown on Si(111) by metalorganic chemical vapor deposition using an AlN buffer layer", ***MRS Internet journal of nitride semiconductor research,*** (2014).

[13] Çörekçi S., Öztürk M., Akaoğlu B., Çakmak M., Özçelik S., "Structural, morphological, and optical properties of AlGaN/GaN heterostructures with AlN buffer and interlayer", ***Journal of Applied Physics,*** 101: 123502-1-4, (2007).

[14] Cörekçi S., Dugan S., Ozturk M., Cetin S., Cakmak M., Ozcelik S., Ozbay E., "Characterization of AlInN/AlN/GaN Heterostructures with Different AlN Buffer Thickness", ***Journal of Electronic Materials,*** 45: 3278-3284, (2016).

[15] Moram M., Vickers E., "X-ray diffraction of III-nitrides", ***Rep Prog Physics,*** 72: 1-40, (2009).

[16] Chierchia R., Wttcher T., Heinke H., Einfeldt S., Figge S., Hommel D., "Microstructure of heteroepitaxial GaN revealed by x-ray diffraction", ***Journal of Applied Physics,*** 93: 8918-8925, (2003).

[17] Arslan E., Demirel P., Çakmak H., Öztürk M., Ozbay E., "Mosaic Structure Characterization of the AlInN Layer Grown on Sapphire Substrate", ***Advances in Materials Science and Engineering,*** 1-11, (2014).

[18] Bas Y., Demirel., Akın N., Baskose C., Ozen Y., Kınacı B., Ozturk M., Ozcelik S., Ozbay E., "Microstructural defect properties of InGaN/GaN blue light emitting diode structures", ***Journal of Materials Science: Mater Electron,*** 25: 3924–3932, (2014).

[19] Corekci S., Ozturk M., Cakmak M., Ozcelik S., Ozbay E., "The influence of thickness and ammonia flow rate on the properties of AlN layers", ***Materials Science in Semiconductor Processing,*** 15: 32-36, (2012).

[20] Tamer M., Ozturk M., Corekci S., Bas Y., Gultekin A., Kurtulus G., Ozcelik S., Ozbay E., "Structural investigation of AlInN/AlN/GaN heterostructures", ***Journal of Materials Science: Mater Electron,*** 27: 2852-2859, (2016).

[21] Liu B., Zhang R., Xie Z., Lu H., Liu Q., "Microstructure and dislocation of epitaxial InN films revealed by high resolution x-ray diffraction", ***Journal of Applied Physics***, 103: 023504-1-4, (2008).

[22] Morse M., Wu P., Choi S., Kim T., Browm A., Losurdo M., Bruno G., "Structural and optical characterization of GaN heteroepitaxial films on SiC substrates", ***Applied Surface Science***, 253: 232–235, (2006)